APPLIED AND ENVIRONMENTAL MICROBIOLOGY, June 1984, p. 1299–1306
0099-2240/84/061299-08$02.00/0

Vol. 47, No. 6

Models for Mineralization Kinetics with the Variables of Substrate Concentration and Population Density

STEPHEN SIMKINS AND MARTIN ALEXANDER*

Institute for Comparative and Environmental Toxicology and Laboratory of Soil Microbiology, Department of Agronomy, Cornell University, Ithaca, New York 14853

Received 19 December 1983/Accepted 23 March 1984

The rates of mineralization of [^{14}C]benzoate by an induced population of *Pseudomonas* sp. were measured at initial substrate concentrations ranging from 10 ng/ml to 100 μg/ml. Plots of the radioactivity remaining in the culture were fit by nonlinear regression to six kinetic models derived from the Monod equation. These models incorporate only the variables of substrate concentration and cell density. Plots of the mineralization kinetics in cultures containing low, intermediate, and high initial substrate concentrations were well fit by first-order, integrated Monod, and logarithmic kinetics, respectively. Parameters such as maximum specific growth rate, half-saturation constant, and initial population density divided by yield agreed between cultures to within a factor of 3.4. Benzoate mineralization by microorganisms in acclimated sewage was shown to fit logistic (sigmoidal), Monod, and logarithmic kinetics when the compound was added at initial concentrations of 0.1, 1.0, and 10 μg/ml, respectively. The mineralization of 10 μg of benzoate per ml in sewage also followed logarithmic kinetics in the absence of protozoa. It is concluded that much of the diversity in shapes of mineralization curves is a result of the interactions of substrate concentration and population density. Nonlinear regression with models incorporating these variables is a valuable means for analysis of microbial mineralization kinetics.

Several types of curves have been obtained in plots of the disappearance of organic molecules added to samples of natural environments or to pure cultures. On arithmetic axes, such substrate disappearance curves may be concave-up (14, 26), as in first-order kinetics, or concave-down during nearly the entire period of decreasing substrate concentration, or the concentration of substrate or the appearance of product may appear to change linearly with time (25, 26, 28). In natural ecosystems, a variety of factors probably alter the shapes of substrate disappearance curves. These factors may include predation by protozoa (8, 19), the time for induction of the active organisms, the accumulation of toxins produced by other microorganisms, depletion of inorganic nutrients or growth factors (8, 19), the presence of other substrates which may repress utilization of the compound of interest, and binding of the compound to colloidal matter (24, 27). The impacts or interactions of such potentially important factors may make it difficult to predict the kinetics of mineralization or disappearance of a particular substrate.

One approach to establish why substrate disappearance curves have so many different shapes is to seek an omnipresent minimum set of factors affecting the kinetics of biodegradation. In many instances, it is possible that the only factors or variables, at least for substrates that are mineralized, that need to be considered are the concentration of the compound and the abundance of active organisms. This study was designed to determine whether the variety of shapes of substrate disappearance curves could be modeled with only the variables of substrate concentration and population density and the parameters of classical Monod kinetics.

THEORY AND METHODS

Theoretical considerations. Several formulations have been proposed to express the growth dynamics of a population that is limited solely by the concentration of a single substrate (10, 15). However, in the development that follows, it is assumed that Monod kinetics adequately describe the relationship between growth rate and substrate concentration. Monod kinetics are frequently expressed as follows:

$$\mu = \mu_{max} \cdot S/(K_s + S) \quad (1)$$

where $\mu = dB/dt(1/B)$ is the specific growth rate, μ_{max} is the maximum specific growth rate, S is the substrate concentration, K_s is the half-saturation constant for growth, and B is the population density. If the population density changes, an expression describing the relation between changes in population size and concomitant changes in substrate concentration is also necessary. For the theoretical development of this paper, the following equation (18), which is sometimes termed a mass-balance equation (5), will be used:

$$S_0 + qB_0 = S + qB \quad (2)$$

where S_0 is the initial substrate concentration, B_0 is the initial population density, and q is the cell quota or inverse yield. Although q changes markedly with nutrient concentration for substrates such as phosphate (5, 16, 17) and nitrogen (11, 12, 16), it is much less variable when the limiting factor is a carbon source (9). Therefore, as a working approximation, the practice of others (3, 18, 21, 22) who modeled nutrient-limited growth will be followed, and q will be treated as invariant with time and substrate concentration in the theoretical development that follows.

When treated as a constant, q becomes impossible to measure without measuring population density; q is only a useful quantity when exact values of B are desired, and it is not needed when only substrate disappearance is of interest. To emphasize this proposition, qB will be replaced in all equations hereafter with X, which corresponds to the amount of substrate required to produce a population density equal to B. By analogy, X_0 is by definition equal to qB_0.

* Corresponding author.

TABLE 1. Six models for mineralization kinetics with only the variables of substrate concentration and cell density

Model and characteristics	Equation and inequalities
I. Zero order	
Differential form	$-dS/dt = k_1$
Integral form	$S = S_0 - k_1 t$
Derived parameter	$k_1 = \mu_{max} X_0$
Necessary conditions	$X_0 >> S_0$ and $S_0 >> K_s$
II. Monod, no growth	
Differential form	$-dS/dt = k_1 S/(K_s + S)$
Integral form	$K_s \ln(S/S_0) + S - S_0 = -k_1 t$
Derived parameter	$k_1 = \mu_{max} X_0$
Necessary condition	$X_0 >> S_0$
III. First order	
Differential form	$-dS/dt = k_3 S$
Integral form	$S = S_0 \exp(-k_3 t)$
Derived parameter	$k_3 = \mu_{max} X_0 / K_s$
Necessary conditions	$X_0 >> S_0$ and $S_0 << K_s$
IV. Logistic	
Differential form	$-dS/dt = k_4 S(S_0 + X_0 - S)$
Integral form	$S = \dfrac{S_0 + X_0}{1 + (X_0/S_0)\exp[k_4(S_0 + X_0)t]}$
Derived parameter	$k_4 = \mu_{max}/K_s$
Necessary condition	$S_0 << K_s$
V. Monod with growth	
Differential form	$-dS/dt = [\mu_{max} S(S_0 + X_0 - S)]/(K_s + S)$
Integral form	$K_s \ln(S/S_0) = (S_0 + X_0 + K_s)\ln(X/X_0) - (S_0 + X_0)\mu_{max} t$
Derived parameter	None
Necessary condition	None
VI. Logarithmic	
Differential form	$-dS/dt = \mu_{max}(S_0 + X_0 - S)$
Integral form	$S = S_0 + X_0[1 - \exp(\mu_{max} t)]$
Derived parameter	None
Necessary condition	$S_0 >> K_s$

With these substitutions, the Monod equation and the mass-balance equation, respectively, can be rewritten as follows:

$$dX/dt \cdot 1/X = \mu_{max} S/(K_s + S) \quad (3)$$

$$S_0 + X_0 = S + X \quad (4)$$

Equation 4 and its derivative can be solved for X and dX/dt, respectively, and these terms can be substituted into equation 3 to give the following differential equation:

$$-dS/dt = \mu_{max} S(S_0 + X_0 - S)/(K_s + S) \quad (5)$$

The differential form in equation 5 is a general expression of substrate disappearance in a system in which only population densities and substrate concentrations determine the kinetics of degradation. Equation 5 reflects both the linear effect of changes in population density and the nonlinear effect of changes in substrate concentration (in the vicinity of K_s) on the rate of substrate disappearance. Extreme ratios of inoculum density to initial substrate concentration or of substrate concentration to K_s permit equation 5 to be approximated by the five simplified or special forms shown together with the general expression in Table 1. For example, when the initial cell density is much greater than the number of new organisms which could be produced from the substrate present at time zero, i.e., $X_0 >> S_0$, the growth of the population during the course of an experiment becomes insignificant on a proportional basis, and the term $(S_0 + X_0 - S)$ can be approximated as simply X_0, as is done for the first three of the special forms in Table 1. Similarly, when the initial substrate concentration is much greater than the half-saturation constant ($S_0 >> K_s$), most of the substrate will disappear while the uptake systems of the cells are saturated. Therefore, $(K_s + S)$ in equation 5 can be approximated as S until the substrate is nearly exhausted. This simplification is reflected in models I and VI in Table 1. Alternatively, the substrate may initially be present at much less than saturating levels ($S_0 << K_s$), in which case the uptake rate per cell becomes a linear function of substrate concentration, and the denominator of equation 5 is approximately equal to K_s (Table 1, models III and IV). Models I, III, IV, and VI can be derived from non-Monod models if such models saturate at high values of S and are roughly linear when S is close to zero.

Integration details for three of the models in Table 1 have been previously reported (3, 4, 7, 14). All of the differential equations in Table 1 are of the separable type (2). They are solved by isolating all terms involving S (including dS) on one side of the equality and convenient constants and dt on the other side. Definite integration (from S_0 to S on one side

TABLE 2. Partial derivatives of the general and four nonlinear special forms of mineralization kinetics derived from the Monod equation used for nonlinear regression analysis[a]

Model	Partial derivatives
Monod, no growth	$dC/dk_1 = -(1 - \zeta)t/(K_s/S + 1)$ $dC/dK_s = -(1 - \zeta)\ln(S/S_0)/(K_s/S + 1)$ $dC/dS_0 = \zeta + (1 - \zeta)(1 + K_s/S_0)/(K_s/S + 1)$ $dC/d\zeta = S_0 - S$
First order	$dC/dk_3 = -S_0(1 - \zeta)t \exp(-k_3t)$ $dC/dS_0 = \zeta + (1 - \zeta)\exp(-k_3t)$ $dC/d\zeta = S_0[1 - \exp(-k_3t)]$
Logistic	$dC/dk_4 = -(1 - \zeta)[X_0(S_0 + X_0)^2tE]/[S_0(1 + X_0E/S_0)^2]$ $dC/dX_0 = (1 - \zeta)[1 + X_0E/S_0 - E(S_0 + X_0)(X_0k_4t + 1)/S_0]/(1 + X_0E/S_0)^2$ $dC/dS_0 = \zeta + (1 - \zeta)[1 + X_0E/S_0 - X_0E(S_0 + X_0)(k_4t - 1/S_0)/S_0]/(1 + X_0E/S_0)^2$ $dC/d\zeta = S_0 - S$
Monod with growth	$dC/d\mu_{max} = -(1 - \zeta)t/D$ $dC/dK_s = (1 - \zeta)[\ln(X/X_0) - \ln(S/S_0)]/[D(S_0 + X_0)]$ $dC/dX_0 = (1 - \zeta)[(\ln(X/X_0) - \mu_{max}t)/(S_0 + X_0) + (S_0 + X_0 + K_s)(1/X - 1/X_0)/(S_0 + X_0)]/D$ $\frac{dC}{dS_0} = \zeta + (1 - \zeta)\left[\frac{\ln(X/X_0) - \mu_{max}t}{S_0 + X_0} + \frac{K_s/S_0}{(S_0 + X_0)} + \frac{S_0 + X_0 + K_s}{X(S_0 + X_0)}\right]/D$ $dC/d\zeta = S_0 - S$
Logarithmic	$dS/d\mu_{max} = -X_0\, t \cdot \exp(\mu_{max}t)$ $dS/dS_0 = 1$ $dS/dX_0 = 1 - \exp(\mu_{max}t)$

[a] E, X, and D are defined in the text.

and from 0 to t on the other) is then performed on both sides of the equality. Algebraic rearrangement of the resulting equations yields explicit functions of t for S in models I, III, IV, and VI (Table 1), whereas it is possible to obtain only implicit relationships between S and t for models II and V.

The names given to the models in Table 1 in two cases, zero order and first order, are derived from the chemical kinetics they resemble. The names for models II and V refer to the manner in which these expressions were obtained. Model II could also be called Michaelis-Menten kinetics. Models IV and VI bear the names associated with the kinetics of growth that occurs as the substrate disappears. Although logistic growth kinetics are only occasionally encountered in microbiological literature (20), they are well-known in ecology (13).

Medium. The inorganic salts solution contained 0.20 g of $MgSO_4 \cdot 7H_2O$, 20 mg of $CaCl_2 \cdot 2H_2O$, 1.5 g of K_2HPO_4, 0.75 g of KH_2PO_4, 5.0 mmol of NH_4Cl, and 1.0 ml of a 1.0% (wt/vol) $FeCl_3 \cdot 6H_2O$ solution per liter. Reagent grade benzoic acid (obtained from Eastman Kodak Co., Rochester, N.Y.) was neutralized with KOH before use. [*U*-ring-^{14}C]benzoic acid (specific activity, 130 mCi/mmol) was obtained from Amersham Corp. (Arlington Heights, Ill.).

Cultures. Sewage samples from the primary settling tank of the sewage treatment plant of Ithaca, N.Y., were passed through Whatman no. 41 filter paper and used immediately. In some studies, a *Pseudomonas* strain was used. The bacterium, which was similar to *Pseudomonas maltophilia* but required no growth factors, was isolated from sewage. Counts of this organism were made by the spread-plate technique after samples were serially diluted in the salts solution. The counting medium contained 0.02% benzoic acid, 1.5% agar, and the salts solution.

For testing mineralizing activity of the *Pseudomonas* sp., 500 ml of a culture containing 2×10^8 cells and 50 μg of benzoate per ml was incubated for 3 h in 2.0-liter Erlenmeyer flasks at 23°C without shaking. The cells were collected by centrifugation and washed three times in sterile salts solution. The cell density was diluted to 3.3×10^6 cells per ml, and 150-ml portions of this suspension were incubated at 23°C without shaking in 500-ml Erlenmeyer flasks. All flasks received similar amounts of labeled benzoate (1,000 to 1,400 dpm/ml), but the total concentration was varied by changing the amounts of unlabeled benzoate added.

Measurement of mineralization. At regular intervals, 2.5-ml samples were removed from the cultures, and 3 drops of concentrated H_2SO_4 were added. The liquid was vigorously aerated for 5 min with compressed air. Subsamples (1.0 ml) were added to scintillation cocktail contained in vials, and the radioactivity was counted with a liquid scintillation counter (model LS7500; Beckman Instruments, Inc., Irvine, Calif.) for a period of time sufficient to observe at least 4,440 counts (1.5% standard deviation). The scintillation cocktails were 8.0 ml of Liquiscint (National Diagnostics, Inc., Somerville, N.J.) and 7.0 ml of aqueous counting scintillant (Amersham) for the pseudomonad and sewage, respectively.

Data analysis. Nonlinear regression analyses were conducted with an author-written computer program, MARQFIT, which performs fits minimizing least squares to data by the method of Marquardt, as described by Bard (1). The MARQFIT program requires the user to supply a model equation and all of the first partial derivatives of the dependent variable in the model equation with respect to the parameters. The partial derivatives of the five nonlinear model equations used in this study are given in Table 2. In the expressions shown, the terms X, D, and E are defined as follows: $X = X_0 + S_0 - S$, $D = (K_s/S)/(S_0 + X_0) + (S_0 + K_0 + K_s)/[X(S_0 + X_0)]$, and $E = \exp[k_4(S_0 + X_0)t]$. The model equations used in MARQFIT are modified from the forms developed in the theoretical section to account for the failure

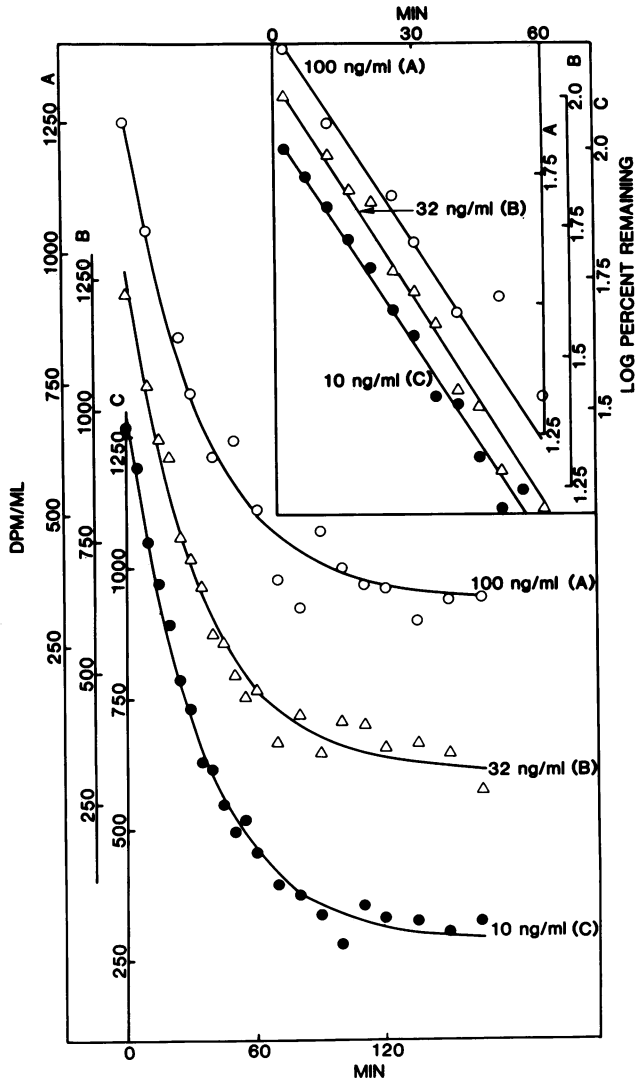

FIG. 1. Patterns of disappearance of radioactivity from solutions containing [^{14}C]benzoate at concentrations of 10, 32, and 100 ng/ml when incubated with the *Pseudomonas* sp. The insert shows the logarithms of the percent benzoate remaining in the first hour. The curves were fit by nonlinear regression.

of the experimental method used to discriminate between counts from parent compound and counts from label incorporated into microbial cells. The modification performed assumes that the ratio between $^{14}CO_2$ and particulate ^{14}C produced during an experiment remains constant; i.e., a constant fraction, ζ, of label taken up is incorporated into the cells. The assumption is equivalent to the decision to treat q as a constant. Given constant ζ, the following equations apply: $C = S + P$ and $P = (S_0 - S)\zeta$ where C represents total counts in the sample, S is counts from the parent compound, S_0 is the number of counts at time zero, and P is counts in the particulate materials. Substituting the second expression into the first results, after algebraic rearrangement, in the following:

$$C = \zeta S_0 + (1 - \zeta)S \quad (6)$$

The general integrated Monod equation and its special forms all can provide a value of S at any given time that can be introduced into equation 6 to give the model equations associated with the partial derivates in Table 2. The partial derivatives of S in the original model equations are modified according to the following scheme to obtain the partial derivatives of C: $dC/d\theta = (1 - \zeta)dS/d\theta$ for all parameters $\theta \neq S_0$; and $dC/dS_0 = \zeta - (1 - \zeta)dS/dS_0$. In addition, a new partial derivative is needed for all models employing ζ: $dC/d\zeta = S_0 - S$. The logarithmic model lacks a horizontal asymptote as t becomes large. Consequently, to compare the values of X_0 generated by this model with those of the other models, they must be corrected, as are values for S in equation 6, with a value for ζ obtained independently.

It is impossible by ordinary means to solve for S in model equations II or V (Table 1). Therefore, these equations were rearranged to the general form $f(S,t) = 0$, and roots of these equations were found numerically in MARQFIT by the method of Newton (2) and substituted into equation 6.

RESULTS

The pseudomonad was incubated with one of each of nine benzoate concentrations, the radioactivity being essentially the same regardless of the total benzoate level in the culture. Plots of the disappearance of radioactivity from solutions containing benzoate at concentrations of 10, 32, and 100 ng/ml are given in Fig. 1. The radioactivity in each instance disappeared rapidly at first, and then the rates declined. Whether the residual radioactivity resulted from the formation of cells or products was not determined. The curves of disappearance of radioactivity from suspensions containing the three lowest benzoate concentrations tested were concave-up and nearly identical.

Benzoate mineralization at the six highest concentrations (0.32, 1.0, 3.2, 10, 32, and 100 μg/ml) is shown in Fig. 2. The disappearance patterns were different from those at the lower substrate concentrations, and some differed among those in the group shown in Fig. 2. The curve at 1.0 μg/ml was concave-up, whereas those at 10, 32, and 100 μg/ml were concave-down.

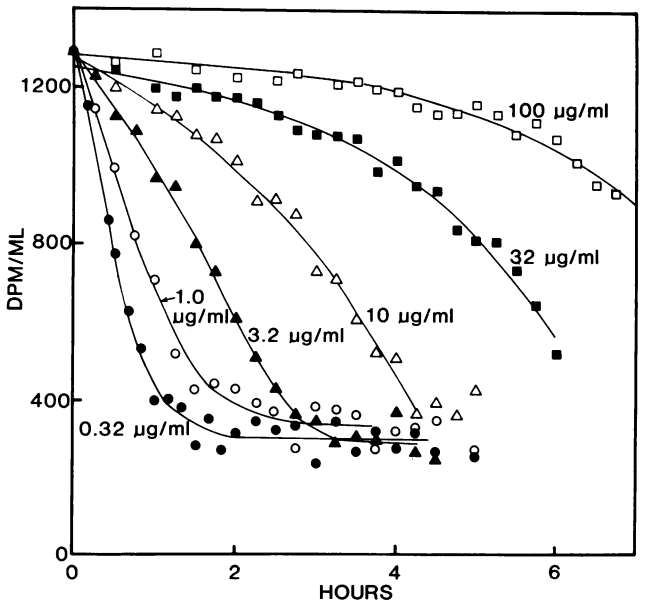

FIG. 2. Patterns of mineralization by the *Pseudomonas* sp. of benzoate at initial concentrations of 0.32, 1.0, 3.2, 10, 32, and 100 μg/ml. The curves were fit by nonlinear regression.

TABLE 3. Parameters and asymptotic standard deviations of four models of substrate disappearance kinetics fit to data on the metabolism of nine concentrations of [*U*-ring-^{14}C]benzoate by the *Pseudomonas* sp.

Actual S_0 (μg/ml)	Model	Rate constant	K_s (μg/ml)	X_0 (μg/ml)	Estimated S_0 (dpm/ml)	
0.010	First order	$k_3 = 0.0290 \pm 0.0009$[a]	NA[b]	NA	1,310 ± 10	0.218 ± 0.006
0.032	First order	$k_3 = 0.0293 \pm 0.0015$[a]	NA	NA	1,260 ± 20	0.244 ± 0.010
0.10	First order	$k_3 = 0.0288 \pm 0.0016$[a]	NA	NA	1,270 ± 30	0.265 ± 0.008
0.32	Monod, no growth	$k_1 = 0.008 \pm 0.002$[c]	0.13 ± 0.07	NA	1,320 ± 30	0.229 ± 0.009
1.0	Monod, no growth	$k_1 = 0.017 \pm 0.005$[c]	0.38 ± 0.25	NA	1,320 ± 30	0.255 ± 0.013
3.2	Monod, growth	$\mu_{max} = 7.2 \pm 0.6$[d]	0.45 ± 0.58	2.1 ± 2.1	1,280 ± 30	0.232 ± 0.0001
10	Logarithmic	$\mu_{max} = 5.6 \pm 0.6$[d]	NA	3.0 ± 0.3	1,270 ± 40	NA
32	Logarithmic	$\mu_{max} = 7.2 \pm 0.5$[d]	NA	1.8 ± 0.3	1,300 ± 20	NA
100	Logarithmic	$\mu_{max} = 7.3 \pm 2.3$[d]	NA	1.8 ± 0.6	1,300 ± 10	NA

[a] First-order rate constant, k_3, with units of minutes^{-1}.
[b] Not applicable.
[c] The constant $k_1 = \mu_{max}X_0$, having units of micrograms per milliliter per minute.
[d] Rate constant for these models is μ_{max} with units of 10^{-3} min^{-1}.

Because the curves at the four lowest concentrations were essentially superimposable, substrate disappearance rates were proportional to benzoate concentration. For this reason and because little growth of the populations would have occurred at the two lowest concentrations (10 and 32 ng/ml), the data from these concentrations were fit to the first-order model. The curves of chemical disappearance at the two highest benzoate concentrations (32 and 100 μg/ml) were fit to the logarithmic model because significant growth of the inoculum was expected and because both concentrations should be well above K_s. The regression estimates for the parameters of the first-order and logarithmic models for the two lowest and two highest initial concentrations, respectively, are given in Table 3. Because the first-order rate constant, k_3, is equal to $\mu_{max} \cdot X_0/K_s$, an estimate for K_s can be calculated as $\mu_{max} \cdot X_0/k_3$, by using the average of the rate constants from the first-order treatments and averages for X_0 and μ_{max} obtained from the logarithmic treatments. The value of K_s thus calculated is 0.45 μg/ml. Given this estimate for K_s, none of the treatments satisfies the condition ($S_0 < K_s$) for the logistic model to be applicable without also satisfying the no-growth requirement of the first-order model. Accordingly, the logistic model was not used in the analysis of any of the results obtained in studies of the *Pseudomonas* sp.

For the five treatments having initial benzoate concentrations of 0.1 to 10 μg/ml, the most appropriate model of those in Table 1 was chosen by a statistical procedure similar to the analysis of variance used in stepwise multiple linear regression to test for the significance of adding an additional independent variable. For example, the first-order model fit the disappearance of 100 ng of benzoate per ml with unexplained variance equal to 42,500 (dpm)^2. Model II (Table 1) (Monod kinetics without growth) also provides a good fit to the disappearance of 100 ng of benzoate per ml, leaving an unexplained variance of 37,100 (dpm)^2. However, the reduction in unexplained variance [5,400 (dpm)^2] obtained by using model II, which has one more parameter than first-order kinetics, is not statistically significant by F-test at the $P = 0.10$ probability level. Therefore, the data from this treatment were analyzed with the first-order model. Model II was used to fit the disappearance of 0.32 and 1.0 μg of benzoate per ml because a statistically significant reduction ($P = 0.01$) in unexplained variance was achieved as compared with the first-order fit, but no further significant decrease (at $P = 0.10$) was obtained with model V (Monod kinetics with growth). Similarly, the disappearance of 10 μg of benzoate per ml was not better fit by model V than by model VI (the logarithmic model). For the disappearance of 3.2 μg of benzoate per ml, model V gave a statistically significant decrease ($P = 0.10$) in unexplained variance as compared with either model II or model VI.

By the criterion described above, estimates were made of the parameters of the model selected as appropriate for cultures incubated with each of the nine concentrations of benzoate. The estimates of derived parameters (defined in Table 1) μ_{max}, K_s, X_0, S_0, and ζ (ζ is the fraction of ^{14}C incorporated into cells) are given in Table 3. Each parameter estimated by nonlinear regression analysis of benzoate disappearance at each concentration can be compared with an estimate of the same parameter independently obtained from at least one other treatment. All such independent estimates

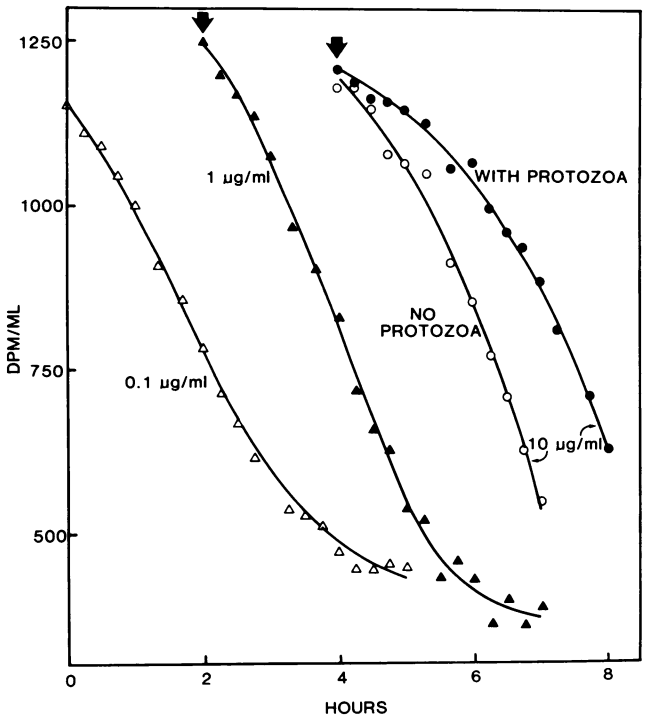

FIG. 3. Mineralization of benzoate added at one of three concentrations to acclimated sewage or filtered, cycloheximide-amended sewage. Curves shown were fit by nonlinear regression.

TABLE 4. Parameters and standard deviations of three models for mineralization kinetics fit to data on the disappearance of benzoate from acclimated sewage with and without protozoa

S_0 (μg/ml)	Protozoa	Model	Rate constant	X_0 (μg/ml)	S_0 (dpm)	ζ
10	Absent	Logarithmic	7.0 ± 0.7[a]	2.2 ± 0.4	1,200 ± 20	NA[b]
10	Present	Logarithmic	7.4 ± 0.4[a]	0.96 ± 0.11	1,210 ± 10	NA
1.0	Present	Monod[c]	17 ± 18[a]	0.27 ± 0.20	1,250 ± 20	0.29 ± 0.02
0.1	Present	Logistic	0.13 ± 0.03[d]	0.022 ± 0.008	1,150 ± 80	0.34 ± 0.03

[a] The rate constant is equal to μ_{max} with units of 10^{-3} min^{-1}.
[b] Not applicable.
[c] The value for the half-saturation constant, K_s, for this model is 0.77 ± 0.96 μg/ml.
[d] The logistic rate constant, k_4, with units of milliliters per minute per microgram.

of a single parameter from different treatments agreed to within approximately half an order of magnitude. The worst agreement between estimates in Table 3 was for K_s values, which differed by as much as a factor of 3.4. The best agreement was for first-order rate constant values, which differed between treatments by <2%. In addition, the rate constants, k_2 and k_3, used in models II and III are themselves products or quotients of parameters such as μ_{max}, K_s, and X_0, which are independently estimated in other treatments. As discussed previously, a value for K_s of 0.45 μg/ml can be calculated from independent estimates of μ_{max}, X_0, and the first-order rate constant; this value is equal to the K_s value found by nonlinear regression analysis of the disappearance of 3.2 μg of benzoate per ml. Because $K_1 = \mu_{max} X_0$ and $k_3 = \mu_{max} X_0/K_s$, another independent estimate of K_s can be obtained from averages of values from fits using these two rate constants (as $K_s = k_1/k_3$); the value so obtained is 0.45 μg/ml, which is identical to the previous estimate made using data obtained from tests of cultures some of which were incubated with different benzoate concentrations.

The curves of best fit in Fig. 1 and 2 were drawn by using the parameter estimates and models in Table 3.

Unlabeled benzoate added at 0.1, 1.0, and 10 μg/ml was added to 150-ml portions of freshly collected, aerated primary sewage contained in 500-ml Erlenmeyer flasks. The flasks were incubated for 48 h at 23°C with aeration provided by bubbling air through the liquid, and a second equal amount of benzoate containing a constant trace amount of ^{14}C-labeled benzoate was then added. Mineralization was then determined by measuring the disappearance of radioactivity from the mixture.

Three different patterns of benzoate mineralization were noted when 0.1, 1.0, and 10 μg of the compound per ml were added to sewage (Fig. 3). The kinetics of mineralization of 10 μg/ml was completely concave-down. Consequently, a fit was made to the logarithmic model. Because the pattern of disappearance of 0.1 μg of benzoate per ml resembled an S-shaped curve symmetric about its inflection point, the logistic model was fit to these data. The curve for the mineralization of 1.0 μg of benzoate per ml had a more complicated shape than that observed for the other two concentrations, and accordingly, these results were analyzed with the integrated form of the Monod equation with growth (model V).

A portion of sewage was treated as above for the 10-μg/ml amendment, but it was also passed through a 3-μm Nuclepore membrane filter and amended with 25 μg of cycloheximide per ml about 1 h after collection. Microscopic examination showed that fewer than 100 protozoa per ml were present 5 days after collection, whereas unfiltered sewage amended with each of the three benzoate levels but no cycloheximide contained more than 10^5 protozoa per ml. The mineralization of 10 μg of [^{14}C]benzoate per ml in both the protozoa-free as well as the protozoa-containing suspensions is shown in Fig. 3. The shapes of the curves reflecting mineralization of 10 μg of benzoate per ml in protozoa-containing suspensions appeared to be the same as in protozoa-free sewage, and the data were, accordingly, analyzed with the same model (model VI).

The coefficients found by nonlinear regression for the experiments with sewage are given in Table 4. Included also are the standard deviations estimated by MARQFIT for each parameter. The values for μ_{max} in sewage receiving 10 μg of benzoate per ml are nearly equal to those found for the *Pseudomonas* sp. (Table 3). The K_s value in sewage receiving 1.0 μg of benzoate per ml is only three times greater than the values calculated for the *Pseudomonas* sp. The kinetic

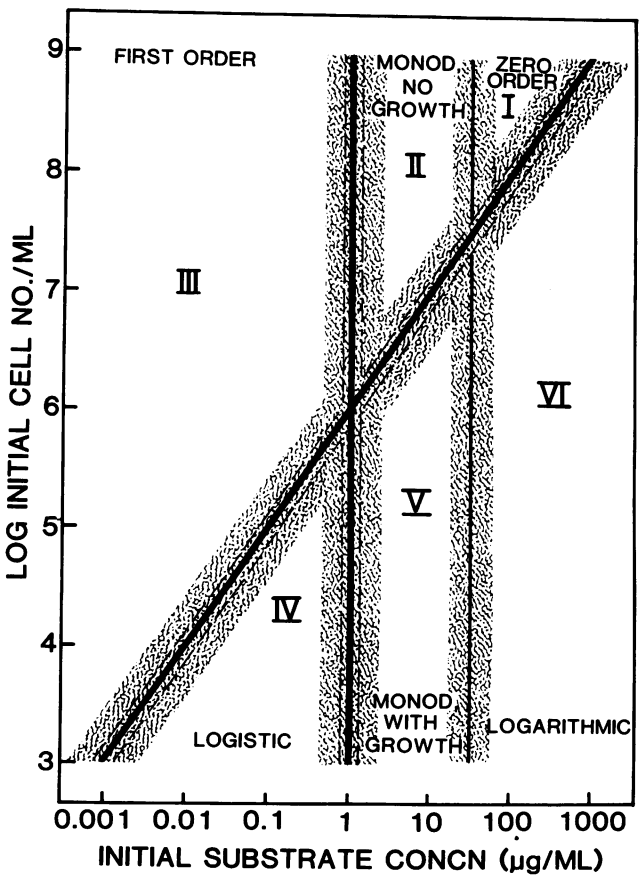

FIG. 4. Applicability of six kinetic models as a function of initial substrate concentration and cell density.

parameters estimated for the protozoa-free and protozoa-containing sewage amended with 10 μg of benzoate per ml differed significantly only in the values for X_0; i.e., time-zero population density divided by yield. Based on the estimated values of X_0, the flasks with protozoa had an estimated population size at the time of [^{14}C]benzoate addition roughly half that of flasks without protozoa.

DISCUSSION

Either the general or one of the special forms of Monod kinetics always provided a close fit to the data obtained in studies of the *Pseudomonas* sp. and sewage. The agreement observed for independent estimates of the same parameter among different treatments argues for the appropriateness of the use of these six models, which incorporate only the variables of substrate concentration and cell density, as a family for describing mineralization in these experiments. Moreover, a particular model from among the six was chosen by an unambiguous statistical procedure for the analysis of mineralization in different treatments according to a logical pattern.

The conditions under which the six models apply can be visualized in terms of a range of initial substrate concentrations and cell densities (Fig. 4). For the purposes of the figure, it is assumed that q (the amount of substrate needed for the formation of one cell) equals 1 pg per cell and K_s = 1.0 μg/ml, but the same trends would apply for other values of q and K_s. Points along the diagonal line correspond to inoculum sizes permitting one division of the active cells at various initial substrate concentrations. If the initial cell density for a test substrate concentration is above this line, population density can be treated as approximately constant. The vertical line at a concentration of 1.0 μg/ml is at the K_s assumed for this visualization. The second vertical line placed on the figure at a concentration approximately one and a half orders of magnitude greater than K_s separates circumstances in which the uptake systems of the active organisms are effectively saturated until the substrate is nearly exhausted from situations in which the reaction rate per cell varies appreciably with substrate concentration. Based on the single diagonal and two vertical lines, the approximate ranges of initial substrate concentrations and cell densities that should show mineralization kinetics corresponding to six models can be predicted. For other substrates, populations, or communities, the figure and the slope would be identical, but the concentrations at which the vertical lines are placed and the vertical intercept of the diagonal would need to be modified. The exact locations of the boundaries between the regions are uncertain and may vary with the precision of the methods used. In the present study, the boundary between regions II and III was placed at $S_0 = K_s$ because the tests in which the benzoate level provided to the *Pseudomonas* sp. was below K_s fit the first-order model; i.e., model III. The diagonal was located based on the data obtained in studies of the mineralization of 1.0 and 3.2 μg of benzoate per ml. Given that plate counts at the start showed the presence of 3×10^6 cells per ml and $qB_0 = X_0$ = 2 μg/ml from the regression estimates, it is possible to calculate q = 0.67 pg per cell. Therefore, the cells initially present should not have doubled in the presence of 1.0 μg of benzoate per ml but should have slightly more than doubled in the presence of 3.2 μg/ml. The division between regions V and VI was drawn as shown because the disappearance of 10 μg of benzoate per ml, a concentration approximately one and a half orders of magnitude greater than K_s, was not significantly better described by the Monod model with growth (model V) than by the simpler logarithmic model (model I).

That upper and lower boundaries for region V should exist is a postulate consonant with the results of Robinson and Tiedje (18) from inspection of the partial derivatives of the integrated Monod equation. They observed highly correlated estimates of some of the parameters of Monod kinetics at substrate concentrations 50 times smaller than or greater than K_s (conditions where models III or VI should apply), whereas at $S_0 = 4K_s$, more independent estimates were obtained. Moreover, the excellent fit they report of the integrated Monod equation (model V) to the disappearance of H_2 used by the *Desulfovibrio* sp. was obtained in tests in which the initial substrate concentration was approximately 13 times greater than K_s.

Either the integrated Monod equation or one of the other models gave good fits to the curves for benzoate mineralization in sewage. In addition, the shapes of the curves for mineralization in sewage having different initial benzoate concentrations were in accord with expectations. The kinetics of mineralization of 10 μg of benzoate per ml fit the logarithmic model. If $K_s \simeq 1$ μg/ml, then the necessary condition ($S_0 >> K_s$) for the logarithmic model to apply is approached in sewage receiving 10 μg of benzoate per ml, and the observed kinetics are in general agreement with theory. Expressing the patterns of mineralization of 1.0 μg of benzoate per ml required the use of the integrated Monod equation because the substrate concentration was of the same order of magnitude as K_s. At relatively low initial population densities (i.e., $X_0 < S_0$) and initial substrate concentrations below K_s, as in the test with 0.1 μg of benzoate per ml, the logistic pattern would be expected.

The six patterns of kinetics can be used in analyses of the impact of different treatments on mineralization. An example is the study of the effects of protozoa in sewage. When the data for mineralization in the presence and absence of protozoa were fit to the logarithmic model, the parameters estimated by nonlinear regression indicated that nearly all the differences observed between the two curves could be explained as resulting from a twofold greater initial number of active bacteria in the latter instance; i.e., X_0 in the presence of protozoa was estimated to be half of X_0 in their absence.

The models discussed here have several limitations. One limitation of all six models is the assumption of constant cell yield with time. Although this is often approximately true for carbon sources (9), exceptions are known. Harrison and Loveless (6) found that the yield, expressed on a dry-weight basis, of *Klebsiella aerogenes* in glucose-limited chemostats was maximal at a specific growth rate of 0.6 h^{-1} and declined by 30% at the lowest dilution rates and by 50% at the highest dilution rates tested. Similarly, Stouthamer and Bettenhaussen (23) found that the yield of another bacterium on glucose varied by as much as a factor of 5 from the lowest to the highest dilution rates. A second limitation of these models is their inapplicability to activity of populations requiring significant induction before the onset of rapid mineralization (7, 15, 18). However, if their limitations are taken into account, these six types of kinetics represent a related family of curves, at least one of which should be capable of describing mineralization in systems in which kinetics are determined solely by population density and substrate concentration.

ACKNOWLEDGMENTS

This research was supported by Public Health Service training grant no. ES-07052 from the Division of Environmental Health

Sciences, National Institutes of Health, and by a grant from the Army Research Office.

LITERATURE CITED

1. **Bard, Y.** 1974. Nonlinear parameter estimation. Academic Press, Inc., New York.
2. **Braun, M.** 1978. Differential equations and their applications. Springer-Verlag, Inc., New York.
3. **Caperon, J.** 1967. Population growth in micro-organisms limited by food supply. Ecology **48**:715–722.
4. **Counotte, G. H. M., and R. A. Prins.** 1979. Calculation of K_m and V_{max} from substrate concentration versus time plot. Appl. Environ. Microbiol. **38**:758–760.
5. **Goldman, J. C.** 1977. Steady state growth of phytoplankton in continuous culture: comparison of internal and external nutrient equations. J. Phycol. **13**:251–258.
6. **Harrison, D. E. F., and J. E. Loveless.** 1971. The effect of growth conditions on respiratory activity and growth efficiency in facultative anaerobes grown in chemostat culture. J. Gen. Microbiol. **68**:35–43.
7. **Hinshelwood, C. N.** 1946. The chemical kinetics of the bacterial cell. Oxford University Press, London.
8. **Huang, T.-C., M.-C. Chang, and M. Alexander.** 1981. Effect of protozoa on bacterial degradation of an aromatic compound. Appl. Environ. Microbiol. **41**:229–232.
9. **Koch, A. L.** 1979. Microbial growth in low concentrations of nutrients, p. 261–279. *In* M. Shilo (ed.), Strategies of microbial life in extreme environments. Verlag Chemie, GmbH, Weinheim, Federal Republic of Germany.
10. **Koch, A. L.** 1982. Multistep kinetics: choice of models for the growth of bacteria. J. Theor. Biol. **98**:401–417.
11. **Maske, H.** 1982. Ammonium-limited continuous cultures of *Skeletonema costatum* in steady and transitional state: experimental results and model simulations. J. Mar. Biol. Assoc. U.K. **62**:919–943.
12. **Mateles, R. I., D. Y. Ryu, and T. Yasuda.** 1965. Measurement of unsteady state growth rates of micro-organisms. Nature (London) **208**:263–265.
13. **Odum, E. P.** 1971. Fundamentals of ecology. The W. B. Saunders Co., Philadelphia.
14. **Paris, D. F., W. C. Steen, G. L. Baughman, and J. T. Barnett, Jr.** 1981. Second-order model to predict microbial degradation of organic compounds in natural waters. Appl. Environ. Microbiol. **41**:603–609.
15. **Powell, E. O.** 1967. The growth rate of microorganisms as a function of substrate concentration, p. 34–56. *In* E. O. Powell, C. G. T. Evans, R. E. Strange, and D. W. Tempest (ed.), Microbial physiology and continuous culture. Her Majesty's Stationery Office, London.
16. **Rhee, G.-Y.** 1974. Phosphate uptake under nitrate limitation by *Scenedesmus* sp. and its ecological implications. J. Phycol. **10**:470–475.
17. **Robertson, B. R., and D. K. Button.** 1979. Phosphate-limited continuous culture of *Rhodotorula rubra*: kinetics of transport, leakage, and growth. J. Bacteriol. **138**:884–895.
18. **Robinson, J. A., and J. M. Tiedje.** 1983. Nonlinear estimation of Monod growth kinetic parameters from a single substrate depletion curve. Appl. Environ. Microbiol. **45**:1453–1458.
19. **Sinclair, J. L., J. F. McClellan, and D. C. Coleman.** 1981. Nitrogen mineralization by *Acanthamoeba polyphaga* in grazed *Pseudomonas paucimobilis* populations. Appl. Environ. Microbiol. **42**:667–671.
20. **Slater, J. H.** 1979. Microbial population and community dynamics, p. 45–63. *In* J. M. Lynch and N. J. Poole (ed.), Microbial ecology: a conceptual approach. Blackwell Scientific Publications, Ltd., Oxford.
21. **Smouse, P. E.** 1980. Mathematical models for continuous culture growth dynamics of mixed populations subsisting on a heterogenous resource base. I. Simple competition. Theor. Popul. Biol. **17**:16–36.
22. **Stewart, F. M., and B. R. Levin.** 1973. Partitioning of resources and the outcome of interspecific competition: a model and some general considerations. Am. Nat. **107**:171–198.
23. **Stouthamer, A. H., and C. Bettenhaussen.** 1973. Utilization of energy for growth and maintenance in continuous and batch cultures of microorganisms. Biochim. Biophys. Acta **301**:53–70.
24. **Subba-Rao, R. V., and M. Alexander.** 1982. Effect of sorption on mineralization of low concentrations of aromatic compounds in lake water samples. Appl. Environ. Microbiol. **44**:659–668.
25. **Subba-Rao, R. V., H. E. Rubin, and M. Alexander.** 1982. Kinetics and extent of mineralization of organic chemicals at trace levels in freshwater and sewage. Appl. Environ. Microbiol. **43**:1139–1150.
26. **Vashon, R. D., and B. S. Schwab.** 1982. Mineralization of linear alcohol ethoxylates and linear alcohol ethoxy sulfates at trace concentrations in estuarine water. Environ. Sci. Technol. **16**:433–436.
27. **Wszolek, P. C., and M. Alexander.** 1979. Effect of desorption rate on the biodegradation of *n*-alkylamines bound to clay. J. Agric. Food Chem. **27**:410–414.
28. **Yordy, J. R., and M. Alexander.** 1980. Microbial metabolism of *N*-nitrosodiethanolamine in lake water and sewage. Appl. Environ. Microbiol. **39**:559–565.